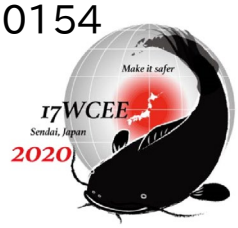

17th World Conference on Earthquake Engineering, 17WCEE
Sendai, Japan - September 13th to 18th 2020

EXPERIMENTAL AND ANALYTICAL EVALUATION OF BASE-ISOLATED BUILDINGS DURING COLLISION

H. Fukui[1], H. Fujitani[2], Y. Mukai[3], M. Ito[4], G. Mosqueda[5]

[1] *Ph.D. student, Kobe University, 153t049t@stu.kobe-u.ac.jp*
[2] *Professor, Kobe University, fujitani@kobe-u.ac.jp*
[3] *Associate Professor, Kobe University, ymukai@port.kobe-u.ac.jp*
[4] *Senior Research Engineer, Building Research Institute, mai_ito@kenken.go.jp*
[5] *Professor, University of California, San Diego, gmosqueda@eng.ucsd.edu*

Abstract

In this study, collision tests using a shaking table were conducted to assess the collision of a base-isolated model specimen with a retaining wall. Input waves were scaled to various amplitudes to examine effects of pounding on the superstructure using different collision velocities. To investigate various values of wall rigidity, the retaining wall was installed as a hard-metal stopper with steel or rubber members attached to its surface. The collision effects on the superstructure were investigated using the relative story displacement and the floor acceleration and impact force of the structure measured through the collision.

An original numerical simulation method using impulse input on the first floor was proposed. The maximum floor acceleration and maximum story shear force of the superstructure during the collision can be evaluated easily using the proposed method, while obviating a collision analysis model.

Findings can be summarized as explained below.

1) The maximum story shear force, the maximum floor acceleration, and the maximum impact force during a collision have an almost linear relation with collision velocity. The maximum floor acceleration and impact force depend on the wall rigidity, whereas the maximum story shear force depends less on wall rigidity.

2) By calculating the impulse using the first floor impact force measured for a load cell, results demonstrated that the impulse depends less on the wall rigidity because, although the impact force increases, the impact duration decreases concomitantly with increased wall rigidity. The story shear force depends less on wall rigidity during the collision, probably because the impulse has a similar value irrespective of the wall rigidity. Therefore, results show that the story shear force and impulse during the collision are closely related.

3) The proposed method uses numerical simulation by inputting a triangle wave force with the same value as the impulse generated at the time of collision to the first floor during the time history analysis. The maximum floor acceleration and maximum story shear force obtained using this method show good agreement with experimentally obtained results. This numerical simulation method can predict the maximum response of superstructure easily during a collision when using only a simple MDOF model without using collision analysis, which requires consideration of backfill soil, wall rigidity, and other effects.

Keywords: *Base-isolated structure, Collision, Impulse, Numerical simulation, Shaking table test*

1. Introduction

Effectiveness of base-isolated systems has been demonstrated for structural designs intended to minimize damage to building superstructures during earthquakes. However, when the base-isolated story deformation exceeds the design considerations during extreme earthquake ground motions, a superstructure might collide with a displacement-limiting device such as the surrounding retaining wall. Evaluation of this scenario requires elucidation of superstructure behaviors when a base-isolated building collides with a retaining wall. In Japan, 300-mm deformations were observed in the base-isolated story of a building in Kushiro city during the 2003 Tokachi-Oki Earthquake [1] having a design deformation clearance of 550 mm. Recently, a 460-mm deformation was observed for a hospital of a base-isolated building in Kumamoto Prefecture during the 2016 Kumamoto Earthquake [2], which had a design deformation clearance of 550 mm. For the U.S., one report described collision of a base-isolated building during the 1994 Northridge Earthquake [3–5] that amplified the building response. However, the result of this case was collision with an obstruction that was closer to the building than the rated clearance. No report of the relevant literature describes a full collision of an actual base-isolated building, although large deformation in base-isolated systems has been reported. In light of increasing concern about the performance degradation of base-isolated buildings under strong earthquakes [6], several analytical and experimental studies have examined collisions between base-isolated buildings and retaining walls [7–12]. Nevertheless, base-isolated structure behavior during a collision has not been sufficiently clarified.

For this study, a shaking table was used to conduct collision tests with a base-isolated model specimen with a retaining wall [13]. The influence of collision on the superstructure was investigated by consideration of the relative story displacements, the floor accelerations, and impact forces measured on the base-isolated building specimen during the collision. A new analysis method using impulse was also proposed to reproduce the measured responses during the collision. The analysis results were compared with experimentally obtained results to validate the numerical model for analysis.

2. Test overview

2.1 Testing model

The dimensions and component configuration of the testing model used for this study are presented in Figure 1. Table 1 presents the testing model specifications. Each floor was supported by flat roller bearings. The restoring force was provided by coil springs. The coil springs exhibited linear characteristics within their available strokes. In the superstructure model shown in Figure 1, each steel floorboard represented the degree of freedom for a shear-building-type model. The coefficient of viscous damping of each story was found using RD method [14]. This study did not consider a friction force of a flat roller because the coefficient of maximum static friction force (μ=0.0037) was sufficiently small as to be negligible.

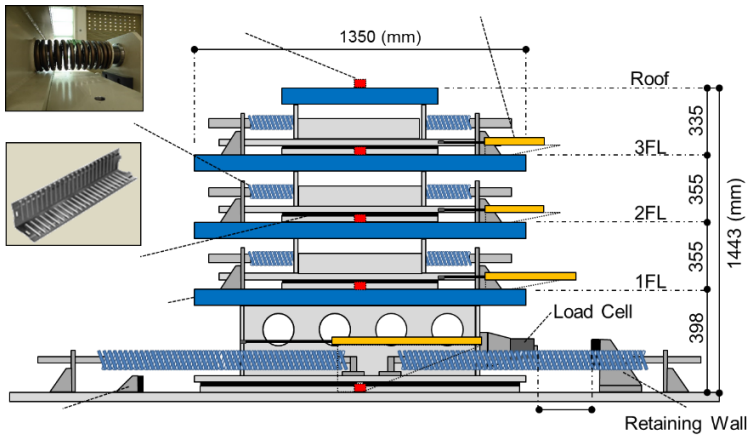

Fig. 1 – Configuration of base-isolated testing model

Table 1 – Structural properties of the testing model

Floor	Mass (kg)	Story	Stiffness (N/mm)	Damping coefficient (N·s/m)
Roof	503.5 (=m_4)	Third	124.3 (=K_3)	1145.2 (=C_3)
3FL	482.2 (=m_3)	Second	119.6 (=K_2)	1622.4 (=C_2)
2FL	478.2 (=m_2)	First	158.7 (=K_1)	1539.5 (=C_1)
1FL	734.8 (=m_1)	Base-isolated	11.6 (=K_b)	430.6 (=C_b)

Natural frequency (Hz)	Mode			
	1st	2nd	3rd	4th
Base-isolated	0.36	1.86	3.66	4.78
Base-fixed	1.19	3.32	4.64	—

2.2 Testing procedure

When the testing model was excited by the shaking table, the load cell attached at the first floor collided with a retaining wall installed with a clearance gap of about 100 mm (Figure 2). The acceleration of each floor, relative story displacement of each story, and the impact force of the first floor were measured using a sampling of 1 kHz. In cases without collision, the retaining wall was removed. In this study, even if there were multiple collisions, only the first collision is reported. During measurements, output signals from accelerometers, displacement transducers, and a load cell were treated with a 100-Hz low-pass filter (LPF) for all. To assess effects on the superstructure while varying the retaining wall rigidity, nitrile rubber (NBR) attached to the retaining wall was changed from hardness of 50°, 70°, 80° and 90°. A compression test was performed on the rubber members based on the measurement method described in the JIS standard (JIS K6254; 2010 5.1 compression test method A). Compressive force-deformation curves were obtained. Table 2 presents the Young's modulus and rigidities for each rubber member calculated from the material test results.

The input ground motions used in these experiments were the following: The NS component of the ground motion observed in Hachinohe port in Japan during the 1968 Tokachi-Oki Earthquake, with the input factor scaled from 35 to 40% by 1% increments (designated as Hachinohe); the NS component of a ground motion observed in El Centro, California during the 1940 Imperial Valley Earthquake, with the input factor scaled from 95 to 107% by 1% increments (designated as El Centro); and the NS component of the ground motion observed at the JR Takatori Railway Station during the South Hyogo Prefecture Earthquake in 1995, by the input factor scaled from 30 to 38% with 1% increments (designated as Takatori). The lower limit of the input factor range is the minimum input at which collision occurs. The upper limit of the input factor range is determined by the system capacity governed by the initiation of uplift in the model. The same input motions were applied in both cases, with and without collisions, for shaking table tests.

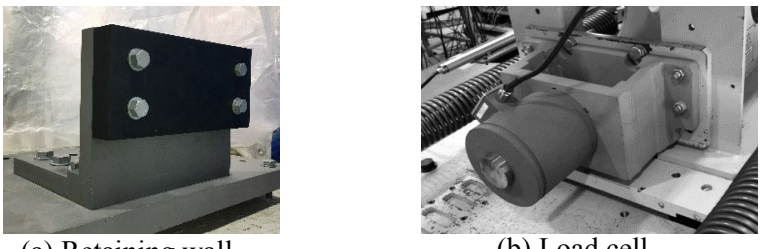

(a) Retaining wall (b) Load cell

Fig. 2 – Photographs of devices at the collision position.

Table 2 – Young's modulus and rigidity of rubber member

	Young's modulus: E (MPa)	Rigidity: K_{rubber} (kN/m)
Hardness 50°	3.69	292.23
Hardness 70°	6.82	540.11
Hardness 80°	18.53	1467.47
Hardness 90°	25.99	2058.26

3. Test results

Figures 3(a)–3(c) portray relations between the collision velocity vs. the maximum story shear force, floor acceleration, and impact force on the first level for all inputs. For the collision cases, the maximum responses were observed from the first peak following the collision. For the cases without collision, the maximum responses were regarded as the first peak values after the relative displacement of the base-isolated story reached the length of the design clearance. Collision velocity was found by the relative velocity of the base-isolated story at the time ($=t_c$) when the relative story displacement exceeded the design clearance and the floor acceleration rapidly increased because of the collision. Figure 4 presents a schematic diagram of the calculation method of the collision velocity. A story shear force F^d was calculated by multiplying the story stiffness by the relative story displacement obtained from the displacement transducer.

Results show that the maximum responses of all kinds have a linear relation with the collision velocity. These results depend less on the difference of input ground motions within the parameters of this experimental study. Furthermore, the maximum floor acceleration and maximum impact force increased as the retaining wall rigidity becomes larger. However, the story shear forces in the superstructure depend less on the difference of the retaining wall rigidity.

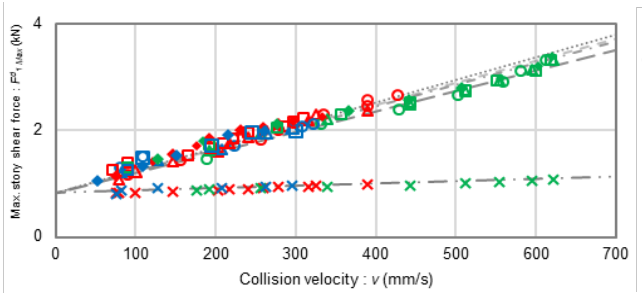

(a) Collision velocity vs. maximum story shear force on first story

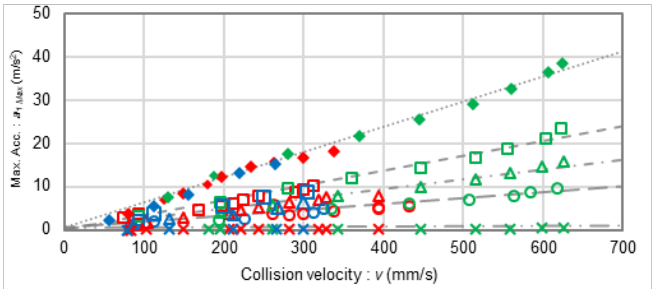

(b) Collision velocity vs. maximum floor acceleration on first floor

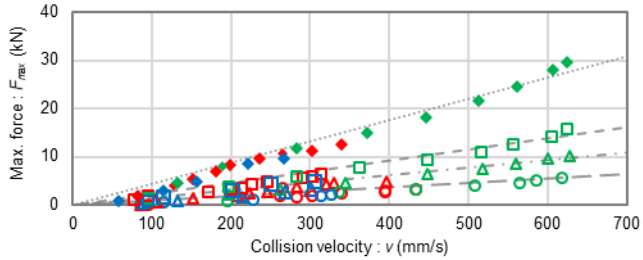

(c) Collision velocity vs. maximum impact force measured by load cell

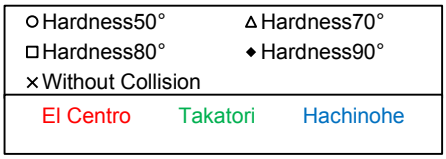

Fig. 3 – Relations between the collision velocity and maximum responses.

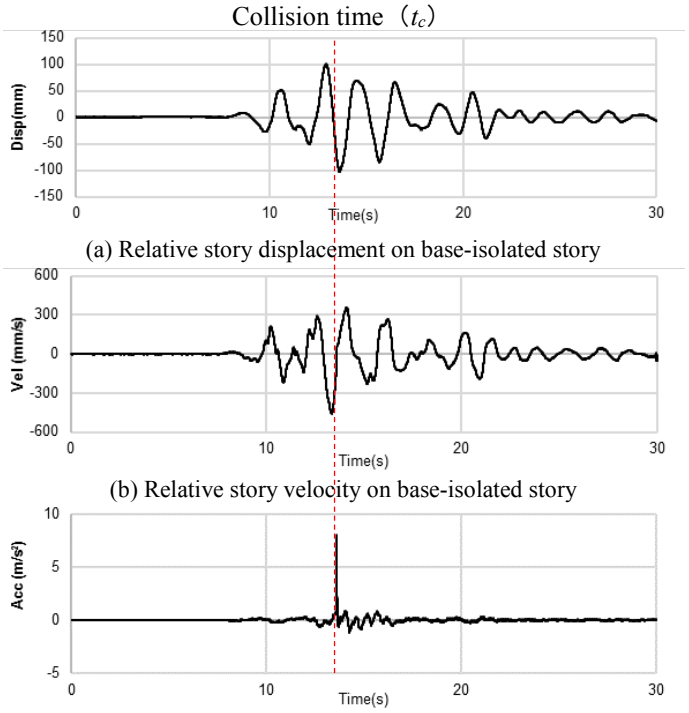

(a) Relative story displacement on base-isolated story

(b) Relative story velocity on base-isolated story

(c) Absolute floor acceleration on first floor

Fig. 4 – Time-history of responses of base-isolated story and first floor (Takatori 30%; hardness 90°; with collision).

4. Story shear force

4.1 Story shear force F^d and F^i

The story shear force was calculated in this study using two methods.

i) The story shear force F^d is calculated by multiplying the story stiffness by the relative story displacement as shown in Equation (1), where K_n represents the stiffness of the *n-th* story, and x_n denotes the relative story displacement of the *n-th* story.

$$F_n^d = K_n \cdot x_n \quad (n = 1,2,3) \tag{1}$$

ii) The story shear force F^i is calculated from the inertial force sum. The inertial forces are calculated by multiplying the floor mass by the floor acceleration when the floor acceleration can be measured directly according to Equation (2), for which m_n signifies the mass of the *n-th* floor, and a_n denotes the floor acceleration of the *n-th* floor.

$$F_{n-1}^i = \sum_n^4 m_n \cdot a_n \quad (n = 2,3,4\ (4: Roof)) \tag{2}$$

Figure 5 presents a comparison of the time-history of the story shear forces F_1^d and F_1^i during Takatori at 38% for cases with and without a collision. In the case without collision, both time-histories of the story shear forces F_1^d and F_1^i showed good agreement. However, in the case with a collision, time histories of the story shear forces F_1^d and F_1^i showed different responses after the collision because of a high-frequency wave included in the story shear force F_1^i

Fourier spectrum analysis was applied to verify the effects of the high-frequency components included in the story shear force F_1^i. Figure 6 presents a comparison of Fourier spectra of the story shear force F_1^d and F_1^i during collision. According to eigenvalue analysis, the natural frequencies of the testing model (spring–mass system) were 0.36 Hz (1st), 1.86 Hz (2nd), 3.66 Hz (3rd), and 4.78 Hz (4th). As Figure 6(a) shows, both Fourier spectra of the story shear force F_1^d and F_1^i had four predominant peaks around these four natural frequencies. These two spectra in the range below about 10 Hz can be regarded as almost identical. However, it was observed that only the spectrum for story shear force F_1^i includes response components at frequencies greater than about 10 Hz, which are frequencies higher than the highest order natural frequency of the test model, as shown in Figure 6(b).

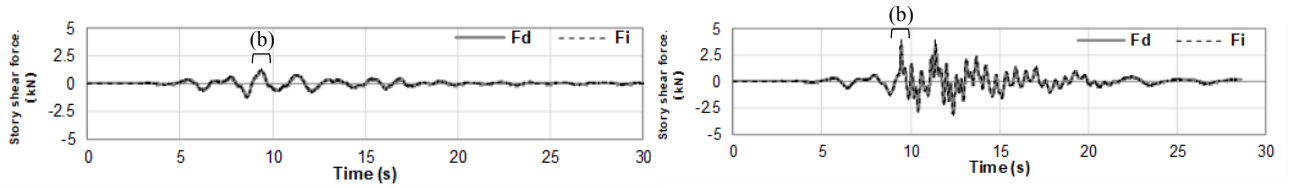

(a) Overall view (0 s – 30 s)

(b) Close view (9.2 s – 9.7 s)

(i) Without collision **(ii) With collision (hardness 90°)**

Fig. 5 – Comparison of time-history of story shear force F^d and F^i on first story (Takatori 38%).

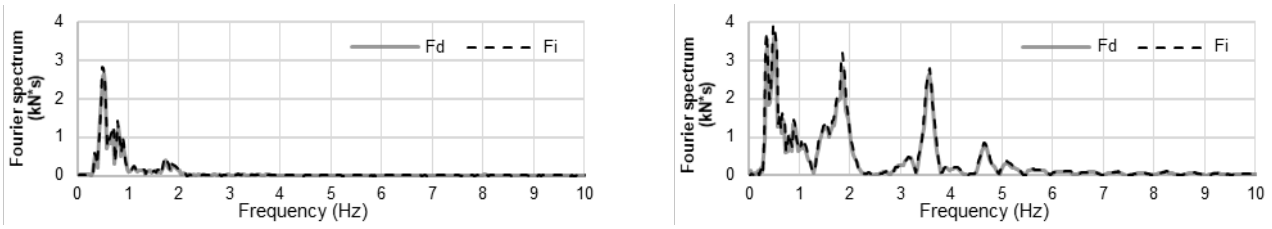

(a) Range of 0 Hz – 10 Hz

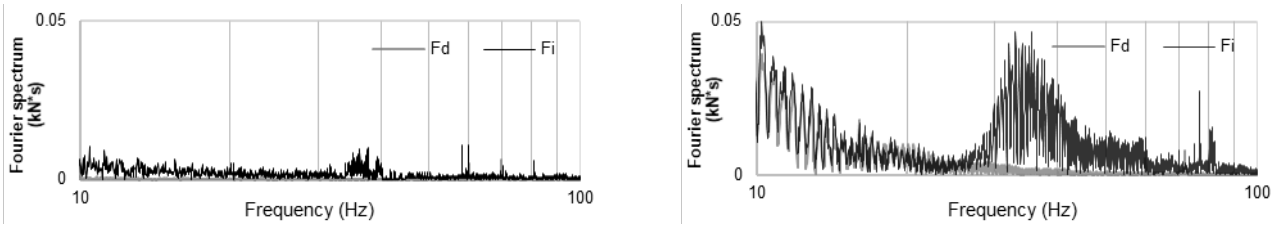

(b) Range of 10 Hz – 100 Hz

(i) Without collision **(ii) With collision (hardness 90°)**

Fig. 6 – Comparison of Fourier spectra of story shear force F^d and F^i on the first story (Takatori 38%).

4.2 High-frequency component

To investigate characteristics of these high-frequency response components in story shear force F^i, the measured acceleration responses at each floor are decomposed into two waveforms in high and low range frequencies at the cut-off frequency of 6 Hz. Considering that the highest natural frequency (4th mode) of the testing model was 4.78 Hz, the acceleration wave was decomposed into low-frequency components and high-frequency components by application of a low or high pass filter (LPF and HPF) with the cutoff frequency of 6 Hz.

Figures 7(a) and 7(b) respectively depict time histories of floor acceleration responses decomposed into high and low ranges at the cut-off frequency of 6 Hz and time histories of floor displacements by integrating the decomposed floor acceleration responses twice. From those figures, we confirmed that high-frequency components did not mostly influence to the response displacement of the testing model during the collision. Consideration of this result indicates that the inertial force calculated from floor acceleration response had large values during a collision because of the high-frequency components included in the floor acceleration. Figure 8 depicts a comparison of the story shear forces F^d and F^i (LPF6 Hz) in the case of a collision using rubber hardness of 90°. Both story shear forces F^d and F^i showed good mutual agreement throughout the test. Using acceleration response filtered out above the range of the highest natural frequency of the testing model, the story shear force calculating by the sum of inertial force F^i during a collision might give the equivalent value for the story shear force F^d by calculating the restoring force using inter-story displacement responses.

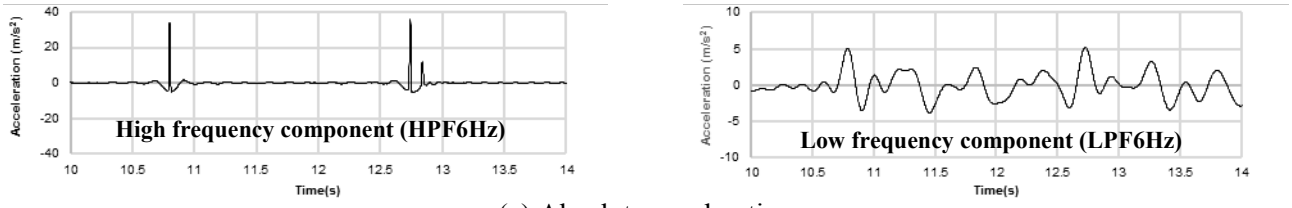

(a) Absolute acceleration

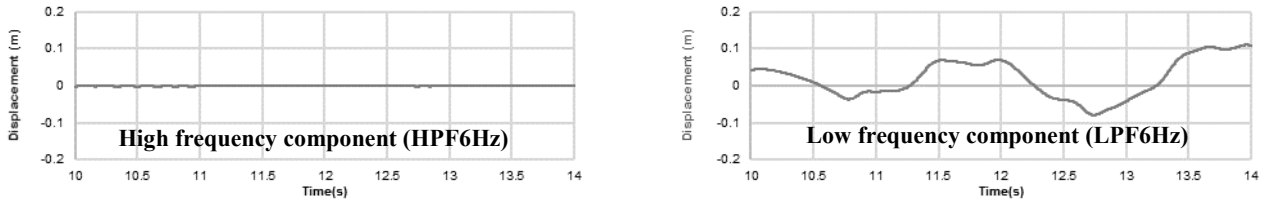

(b) Absolute displacement

Fig. 7 – Time-history of floor acceleration and displacement on the first story (Decomposed into high and low frequencies).

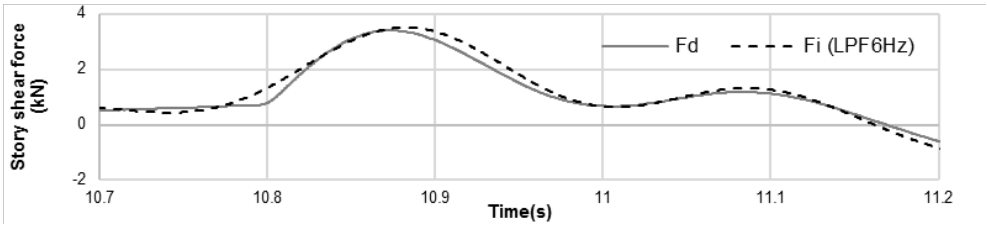

Fig. 8 – Comparison of time-history of story shear force F^d and F^i (LPF6 Hz) on first story (Takatori 38%).

5. Response evaluation of the superstructure using impulse

This section specifically describes the relation between impulse and the superstructure responses. The time-history analysis method using impulse was proposed and verified through comparison between the analytical results and experimentally obtained results. The input ground motions used for investigation in this section are half-sine waves with frequency of 1.6 Hz. The maximum acceleration was 3 m/s^2, with the input factor scaled from 23 to 35% by 1% increments (designated as half-sine). A clearance gap of the base-isolated story was about 100 mm. The sampling time of measurement was 1 kHz.

5.1 Impulse input to the first floor

The impulse input to the first floor was calculated by integrating the impact force measured by the load cell within the colliding time (t). Figure 9(a) depicts a time-history of the impact force measured directly by the load cell. The impulse corresponds to the area in Figure 9(a). However, the impulse is obtainable by multiplying the response acceleration by the mass of the collision object; it is designated as a converted impact force [15]. Figure 9(b) and Table 3 show comparisons between the impact force measured by the load cell and the converted impact force. According to Figure 9(b), both waveforms were observed to be almost identical. Therefore, evaluating the impulse using the converted impact force is inferred to be as effective as measuring the impact force by a load cell. Figure 10 shows the time-history of impact force measured by the load cell colliding with various rubber members. Figure 10 shows why the value of impulse depended less on the difference in wall rigidity. The value of the impulse became constant because the maximum impact force increased as the wall rigidity increased, but the collision time decreased. These results show that the tendency that the story shear force depended less on the wall rigidity, described in Section 3, resulted from the impulse input to the first floor depended less on the wall rigidity. Results suggest that the impulse was involved in the story deformation of the superstructure.

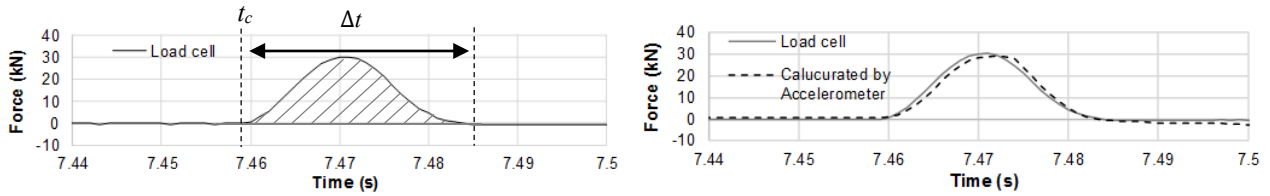

(a) Impact force measured by load cell (b) Impact force measured by load cell and by accelerometer

Fig. 9 – Time history of impact force (half-sine 35%, with collision, hardness 90°).

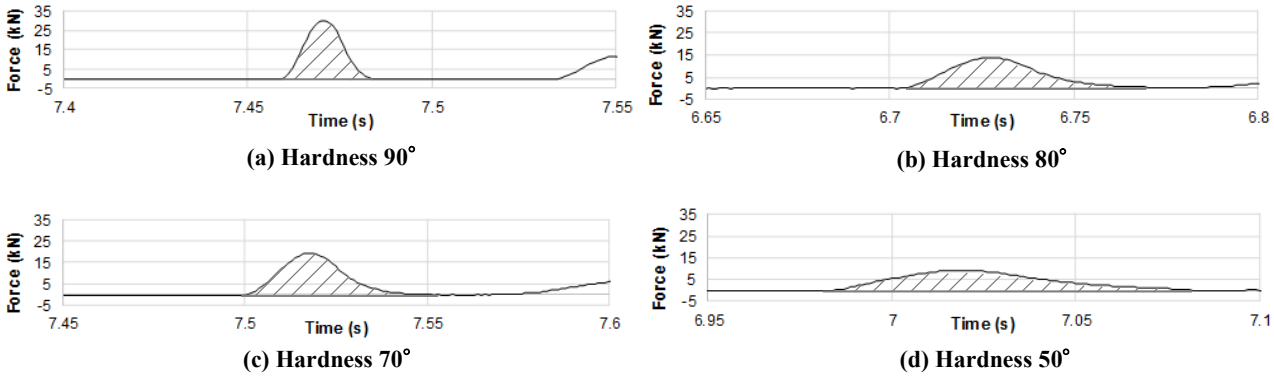

(a) Hardness 90° **(b) Hardness 80°**

(c) Hardness 70° **(d) Hardness 50°**

Fig. 10 – Time history of impact force measured by load cell (half-sine 35%, with collision).

Table 3 – Values of impulse and collision velocity for respective wall rigidities

Input	Hardness 90°			Hardness 80°			Hardness 70°			Hardness 50°		
	Collision velocity (mm/s)	Impulse (kN・s)		Collision velocity (mm/s)	Impulse (kN・s)		Collision velocity (mm/s)	Impulse (kN・s)		Collision velocity (mm/s)	Impulse (kN・s)	
		Load cell	Acceler-ometer		Load cell	Acceler-ometer		Load cell	Acceler-ometer		Load cell	Acceler-ometer
23%	119.3	0.092	0.096	119.1	0.087	0.101	102.4	0.074	0.084	119.7	0.086	0.099
24%	156.4	0.123	0.127	162.7	0.130	0.137	153.0	0.124	0.134	160.9	0.133	0.140
25%	192.3	0.164	0.170	185.4	0.163	0.168	192.7	0.168	0.166	184.1	0.154	0.166
26%	224.9	0.177	0.197	216.9	0.201	0.200	222.3	0.183	0.195	218.6	0.188	0.194
27%	244.4	0.214	0.212	250.2	0.220	0.218	247.7	0.214	0.218	242.0	0.203	0.219
28%	275.7	0.237	0.238	273.0	0.243	0.238	271.5	0.242	0.244	272.9	0.243	0.251
29%	296.6	0.254	0.261	295.8	0.254	0.260	290.7	0.261	0.259	288.1	0.263	0.260
30%	318.3	0.282	0.283	312.6	0.279	0.281	313.8	0.291	0.277	314.5	0.281	0.282
31%	337.9	0.294	0.292	338.5	0.298	0.300	333.9	0.301	0.298	338.3	0.306	0.304
32%	359.4	0.324	0.314	358.0	0.321	0.310	352.3	0.325	0.313	357.2	0.328	0.324
33%	379.4	0.333	0.331	379.4	0.345	0.330	376.2	0.351	0.333	378.0	0.357	0.343
34%	392.6	0.341	0.343	399.2	0.355	0.350	397.2	0.358	0.351	393.7	0.359	0.351
35%	424.2	0.374	0.371	427.4	0.382	0.378	438.5	0.391	0.386	423.2	0.381	0.378

5.2 Time-history analysis method using impulse

From the verification presented in the preceding section, it is considered that the story shear force of the superstructure depends on the impulse input to the first floor. This section proposes a new analytical method to reproduce the superstructure behavior during the collision using input of the impulse to the first-floor mass of the MDOF model (designated herein as "Impulse–input analysis"). The analysis results were verified through comparison with the experimentally obtained result. In this impulse-input analysis method, the impulse input to the first-floor mass was modified to a triangular wave. Figure 11 presents the triangular wave model. The triangular wave area was determined in the same way as a value of impulse calculated in section 5.1. The height of the triangular wave ($=F_{max}$) was found to be a value of the maximum impact force measured by the load cell. The superstructure was modeled as the MDOF model. The time-history analysis was conducted with triangular wave force input to the first-floor mass at the collision time ($=t_c$). Figure 12(a) presents a schematic diagram of the impulse-input analysis.

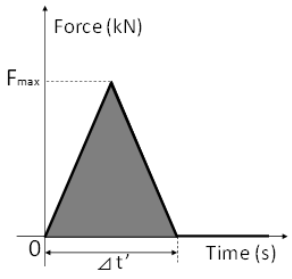

Fig. 11 – Time history of impact force measured by load cell (half-sine 35%, with collision).

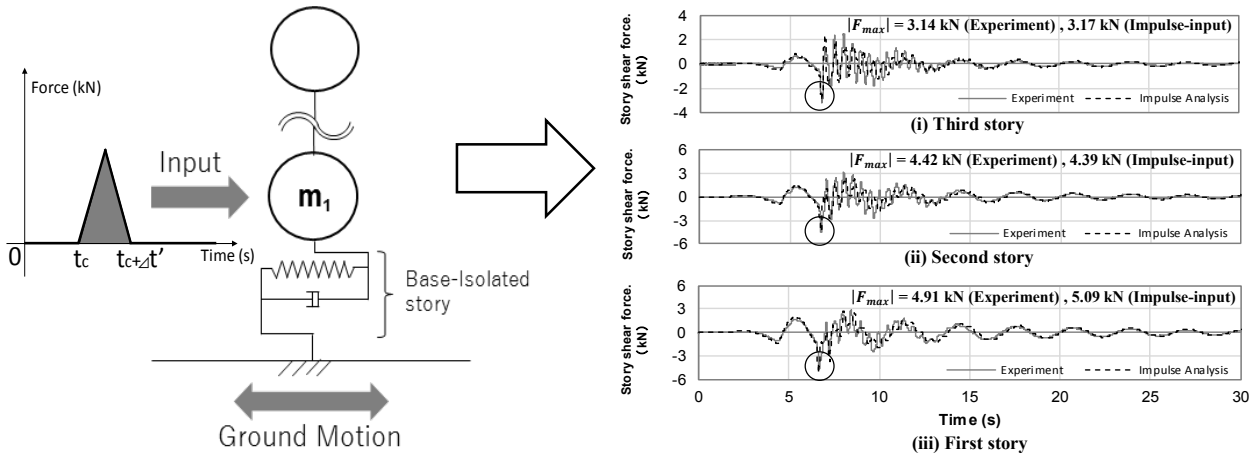

(a) Simulation model

(b) Time-history of story shear force

Fig. 12 – Schematic diagram of impulse-input analysis and comparison of story shear forces found by experimentation and by impulse-input analysis (half-sine 30%, with collision, hardness 90°).

5.3 Comparison of results found through experimentation and impulse-input analysis

Figure 12(b) presents time-history responses of the story shear force F^d for experimental and analytical results during half-sine at 30% with hardness 90°. The triangular wave was found from the value of impulse: 0.282 kN•s, F_{max}=21.2 kN, ($\Delta t'$=0.026 s). Figure 12(b) shows that the impulse-input analysis was able to reproduce the experimental response of the superstructure during the collision. Figure 13 shows maximum values obtained as analysis results and experimentally obtained results for each floor acceleration and each story shear force of the superstructure. Figure 13 plots show the ratio of the maximum value of the analysis results divided by the maximum value of the experimentally obtained results. Figure 13 shows that the difference between the experimentally obtained result and the analytical result is not greater than 20%. These results confirmed that the impulse-input analysis can accurately reproduce the experimental maximum floor response acceleration on each floor and the maximum story shear force on each story during a collision. The impact-input analysis was also able to simulate the tendency by which the maximum floor acceleration becomes high depending on the increased wall rigidity, and the tendency by which the maximum story shear force has less dependence on wall rigidity during the experiment.

Verification results presented in this section confirmed that the time-history analysis using the impulse input to the first-floor mass of the MDOF model can simulate the superstructure behavior during the collision and confirmed that it is useful to predict the maximum response value of the superstructure. This new analytical method is a useful and simple method that obviates modeling of the retaining wall. This analytical method can predict the maximum response of superstructure easily during a collision without using collision analysis. Also, the experimentally obtained results described in section 5.1 indicate that these analytical results reproduced the maximum floor acceleration during the collision depending on the maximum impact force on the first floor and the story shear force of the superstructure depending on the value of the impulse input to the first floor.

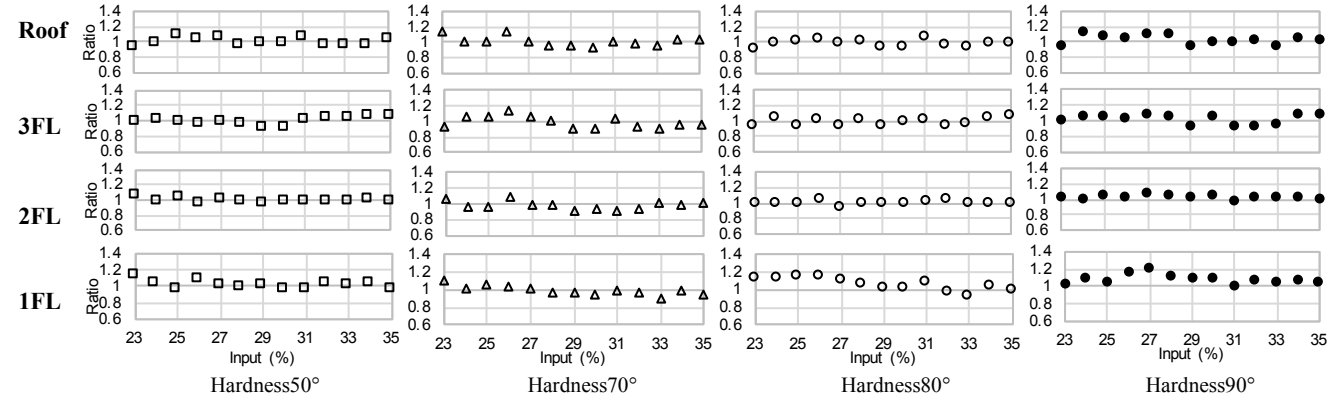

(a) Floor acceleration

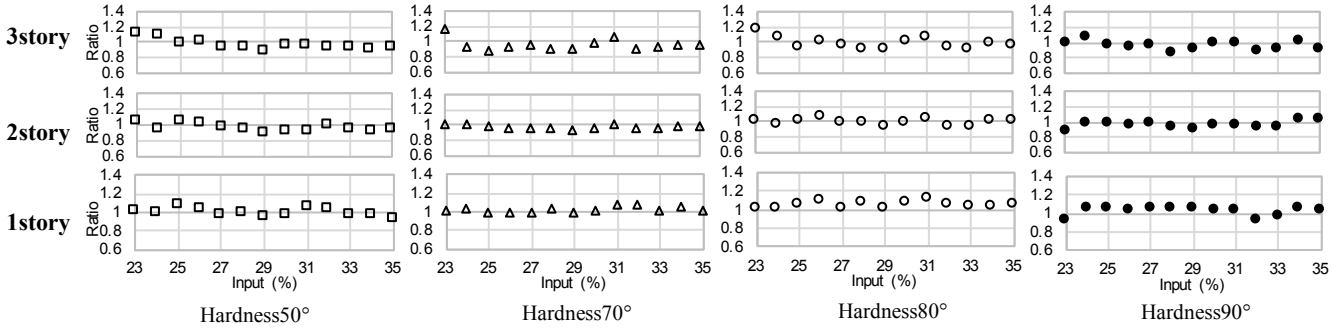

(b) Story shear force

Fig. 13 – Comparison of maximum response values calculated using experiment and impulse-input analysis.

6. Conclusion

This extensive experimental study using a shaking table was conducted to assess collisions of a base-isolated model with a retaining wall. The influence of collision on the superstructure response was investigated using the relative story displacement and the floor acceleration responses of the superstructure and the impact force at the isolated-floor measured through the collision test. The new time history analysis method used impulse input, which can reproduce the superstructure behavior during a collision. The findings can be summarized as explained below.

1) The maximum values of story shear force, floor acceleration, and impact force during a collision respectively exhibit nearly linear relations with collision velocity. The maximum values of floor acceleration and impact force depend on the retaining wall rigidity, although the maximum story shear force depends less on the retaining wall rigidity.
2) The story shear force F^i calculated by summing inertial forces approaches the story shear force F^d calculated using relative story displacement in a case without a collision. However, for cases with collision, the story shear forces F^i and F^d become different because of acceleration responses including high-frequency components. By considering floor acceleration responses filtering out the range over the highest natural frequency of the testing model, both the story shear forces F^i and F^d during a collision become similar values.
3) By calculating the impulse using the first-floor impact force measured using a load cell, results showed that the impulse depended less on wall rigidity. The impact duration decreases with increased wall rigidity, although the impact force increases. Therefore, we infer that the maximum story shear force of the superstructure depends on the impulse. We infer that the maximum floor acceleration depends on the maximum impact force.
4) Results confirmed that the superstructure response during a collision can be well-reproduced using a numerical analysis method that applies the time history of the impulse to the first floor. Results also show

that the maximum floor acceleration and story shear force exhibit good agreement with experimentally obtained results. This new analytical method can predict the maximum response of the superstructure of the base-isolated building easily during a collision without modeling the retaining wall.

Acknowledgments
The part of this study was supported by JSPS grant No. R2904 in the Program for Fostering Globally Talented Researchers and JSPS KAKENHI Grant Number JP 19J12113. The authors express special appreciation to the funding sources.

6. References

[1] Suzuki, Y., Takenaka, Y., Urushizaki, T. and Saito, H.: Behavior of a Base-Isolated Building in Kushiro City for the Tokachi-Oki Earthquake in 2003 (Part 1 and Part 2), *Summaries of Technical Papers of Annual Meeting*, Architectural Institute of Japan, ***B-II***, pp.279–281,2004.7 (in Japanese)

[2] Takayama, M., Morita, K.: A study on the response of seismically isolated hospital in Aso during 2016 Kumamoto earthquake, *Summaries of Technical Papers of Annual Meeting*, Architectural Institute of Japan, ***B-II***, pp.1051-1052, 2017.7 (in Japanese)

[3] Earthquake Engineering Research Institute (EERI): Northridge Earthquake of January 17, 1994 (Preliminary Reconnaissance Report), *Earthquake Engineering Research Institute (EERI)*, 1994.3

[4] Shakal, A., Huang, M., Darragh, R., Cao, T., Sherburne, R., Malhotra, P., Cramer, C., Sydnor, R., Graizer, V., Maldonado, G., Petersen C. and Wampole, J.: CSMIP Strong-Motion Records from the Northridge, *California Earthquake of January 17 1994*, Report No. OSMS. ***94–07***, California Strong Motion Instrumentation Program 1994, Division of Mines and Geology.

[5] Nagarajaiah S., Sun, XH. Base-isolated FCC building: impact response in Northridge earthquake, *Journal of Structural Engineering (ASCE)*, ***127***, pp.1063–1075, 2001.

[6] Mavronicola, EA., Polycarpou, PC., Komodoromos, P.: Spatial seismic modeling of base-isolated buildings pounding against moat walls: effects of ground motion directionality and mass eccentricity, *Earthquake Engineering and Structural Dynamics*, ***46***, pp.1161–1179, 2017.

[7] Komodromos, P., Polycarpou, PC., Papaloizou, L., Phocas, MC.: Response of seismically isolated buildings considering poundings. *Earthquake Engineering and Structural Dynamics*, ***36***, pp.1605–1622, 2007.

[8] Polycarpou, PC., Komodoromos, P., Polycarpou, AC.: A nonlinear impact model for simulating the use of rubber shock absorbers for mitigating the effects of structural pounding during earthquakes, *Earthquake Engineering and Structural Dynamics*, ***42***, pp.81–100, 2013.

[9] Yasumoto, H., Okazawa, R., Takiyama, N., Onishi, Y., and Hayashi, Y.: Maximum Response Evaluation of Base-Isolated Buildings Against Pulse-like Ground Motions in Case of Collision to Retaining Wall. *Journal of Structural and Construction Engineering (Transactions of AIJ)*, ***79***, pp.385–392, 2014. (In Japanese)

[10] Masroor, A., Mosqueda, G.: Impact model for simulation of base isolated buildings impacting flexible moat walls, *Earthquake Engineering and Structural Dynamics*, ***42(3)***, pp.357–376, 2013.

[11] Pant, DR., Wijeyewickrema, AC.: Structural performance of a base-isolated reinforced concrete building subjected to seismic pounding, *Earthquake Engineering and Structural Dynamics*, ***DOI: 10.1002/eqe.2158***, 2012.

[12] Tsai, HC.: Dynamic analysis of base-isolated shear beams bumping against stops, *Earthquake Engineering and Structural Dynamics*, ***26(5)***, pp.515–528, 1997.

[13] Fukui, H., Fujitani, H., Mukai, Y., Ito, M., and Mosqueda, G.: Response evaluation and analysis using impulse of base-isolated building during a collision with retaining wall, *Journal of Structural and Construction Engineering (Transactions of AIJ), **84**, No.766, pp.1533–1543, 2019. (in Japanese)*

[14] Jeary, A.P.: Damping in tall buildings- a mechanism and a predictor, *Earthquake Engineering and Structural Dynamics*, ***14***, 1986.

[15] Kiyoshi, M.: The World of Impulse Destruction, *Transactions of the Institute of Japanese Architects*, **21**, pp.246–251, 1941. (in Japanese)

